Recent Advances in Fiber Cavity Ring-down Technology

Susana Silva and Orlando Frazão

INESC TEC and Department of Physics and Astronomy, Faculty of Sciences of University of Porto,
Rua do Campo Alegre 687, 4169-007 Porto, Portugal

Keywords: Cavity Ring-down, Optical Fibre Sensors, Strain, Curvature, Refractive Index.

Abstract: A brief review in the fibre cavity ring-down (CRD) technique is presented. It addresses the latest developments in CRD technique for sensing applications, undergone at INESC TEC. The CRD is based on the conventional configuration with the possibility of adding amplification in order to compensate the output signal losses induced by the sensing head. The results obtained for strain, curvature and refractive index sensing are presented, corresponding to distinct sensing structures, namely, a chirped fibre Bragg grating (FBG), a long period grating (LPG) and a multimode interference (MMI) based sensor.

1 INTRODUCTION

The cavity ring-down (CRD) technique consists in a spectroscopy method broadly used in technology. Being mainly employed in the sensor area, this methodology enables an accurate analysis of amplitude behaviour over the time. Throughout the past decades, the CRD spectroscopy has been subject of a lot of research, namely in chemical and molecular analysis in real time (Berden *et al.*, 2000). The principle involved settles the basis for various configurations, being also applied to resonant optical cavities with high reflective mirrors, as a result of the high evolution of this technique (Herbelin, 1980) (Herbelin *et al.*, 1980; Anderson *et al.*, 1984). Through association with the previous developed fibre loops, there were implemented new fibre optic-based CRD settings, which, in turn, used a fibre loop operating as the resonant cavity. This configuration quickly obtained a lot of popularity in the scientific community, mainly for presenting an effective alternative to the usual CRD configuration (Stewart, 2004). By virtue of these conceptual studies, the CRD technique has been target of a lot of research in the spectroscopy field, being implemented in the last decade to the measurement of physical parameters, such as strain (Tarsa *et al.*, 2004; Ni *et al.*, 2007; Silva *et al.*, 2015a), temperature (Wang, 2005), curvature (Lerber *et al.*, 2002; Silva *et al.*, 2015b) and pressure (Wang and Scherrer, 2004a; Wang and Scherrer, 2004b; Qiu *et al.*, 2007). More recently, a fast development of CRD technique allied to the biochemical sensing field can also be easily recognized. The implementations in this area are quite extensive, which can go from detection of organic dyes (Brown *et al.*, 2002) to unicellular organisms (Tarsa *et al.*, 2004), or even 1-octyne in decane solution (Pu and Gu, 2009). The CRD approach has also been widely used for refractive index of liquids (Ni *et al.*, 2008; Zhou *et al.*, 2009a; Zhou *et al.*, 2009b; Wang *et al.*, 2010; Wong *et al.*, 2012) and gas sensing (Stewart *et al.*, 2001; Vogler *et al.*, 2003; Zhao *et al.*, 2013; Shimizu and Noriyasu, 2014).

In addition to these applications, the CRD technique use is widespread, being implemented in chemical sensors (Wang, 2009), using frequency-shifted interferometry (Ye *et al.*, 2011), using wavelength-tuneable ultrashort pulsed light (Hiraoka *et al.*, 2013) or even an Optical Time Domain Reflectometer (OTDR) instead of the usual implemented laser and modulator setup (Passos *et al.*, 2014). More recently, a new CRD topology for remote sensing was demonstrated (Silva *et al.*, 2016).

This work adresses the latest developments in fibre optic based CRD technique for sensing applications, undergone at INESC TEC. The results obtained for strain, curvature and refractive index sensing are presented, with focus to the sensing structures used and the CRD configuration for such purpose.

2 FIBER-OPTIC CRD SETUP

The experimental setup of the main configuration CRD system used for sensing is presented in Figure 1. The fibre loop is composed of two standard (2 × 1) 1:99 optical fibre couplers and a sensing head. A commercial OTDR is used as modulated laser source in order to send impulses (1 μs at 1550 nm) down into the fibre cavity. The train of pulses is coupled via 1% arm of the input optical coupler, rings around inside the fibre loop and is coupled out via 1 % arm of the output coupler; the amplitude of the output pulses decay temporally due to the total existing losses in the fibre loop (fibre loss, fibre couplers insertion losses, sensing head transmission attenuation), passes through a photodetector (gain of 40 dB) and is monitored in an oscilloscope.
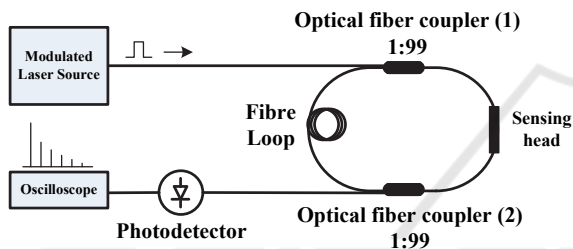

Figure 1: Experimental setup of the CRD configuration that uses an OTDR as laser source and a transmission-based fiber structure as sensing head.

The advantage of using an OTDR is to allow system optimization either in terms of impulse and optical power – allowing its use in long distance applications. Furthermore, the use of a multimode laser source increases the optical power inside the fibre loop. Also, the output signal of the OTDR may be used as laser source or to interrogate the variation of the output signal.

3 SENSING APPLICATIONS

3.1 Strain Sensing

A fibre-based CRD configuration using an OTDR to interrogate the output signal has been developed for the measurement of strain (Silva *et al.*, 2015a). The sensing head, which is placed inside the fibre loop cavity (~1560 m), is based on a chirped fibre Bragg grating (chirped-FBG) and acts as a strain sensing element. The chirped-FBG is centred at 1570 nm, has 4 nm width and is interrogated in transmission.

The output signal response is strongly dependent of the wavelength position of the FBG with respect to the OTDR laser source (operating at 1550 nm). If the chirped-FBG is placed at lower wavelengths, the output signal is expected to decrease with increasing strain. On the other hand, if the FBG is placed at wavelengths higher than 1550 nm (in this case, the FBG is centred at 1570 nm) the output signal is expected to increase with applied strain.

Figure 2 presents the OTDR pulse intensity decay that is back-reflected by the chirped-FBG inside the fibre loop. At the beginning, there is signal saturation that may be avoided by placing a few meters of singlemode fibre between the OTDR and the cavity ring. Afterwards, the amplitude of the signal decays due to the several round trips of the pulse inside the cavity, as expected.
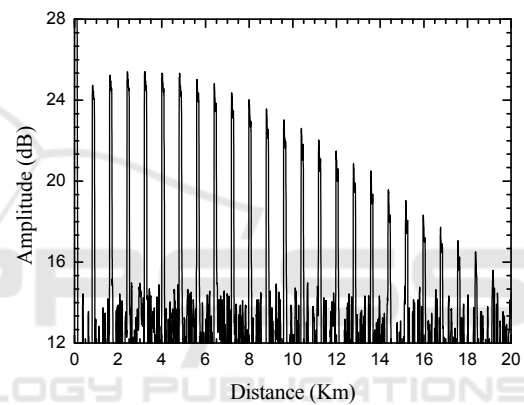

Figure 2: OTDR waveform of the impulse intensity decay caused by the chirped-FBG inside the fiber loop.

The operation mode of the CRD interrogated by the OTDR is based on the second reading of the back-reflected light from the FBG. In this case, the light travelled ca.1600 m which corresponds to a single round trip of 8 μs, similar to the one obtained with the CRD configuration. This also corresponds to the distance between two consecutive peaks (800 m from observing Fig. 2) – due to signal processing of the OTDR, the back-reflected and measured light is divided by 2; therefore, the effective distance between two consecutive peaks is ca. 1600 m.

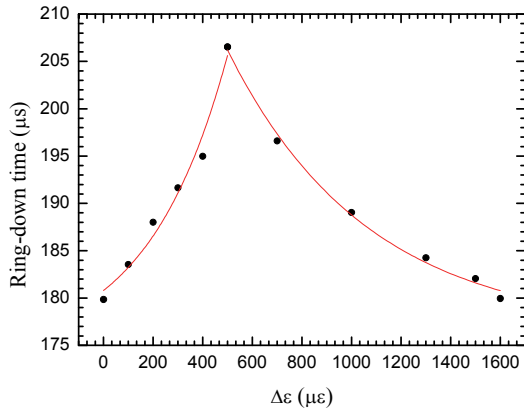The OTDR may also be a viable interrogation method as depicted in Figure 3.

Figure 3: Cavity ring-down time versus applied strain to the chirped-FBG when interrogated by the OTDR.

When strain is applied, the chirped-FBG moves to longer wavelengths, scanning the several wavelength peaks of the laser source and thus resulting in a periodic behaviour as shown in Figure 3. In this case, the ring-down time is almost 10-fold the one obtained with the conventional CRD configuration (22.8 μs) and ranges from 180 to 206 μs due to the FBG position regarding the laser source. Using the CRD configuration it was possible to obtain a linear response to strain applied to the chirped-FBG in the range 0-2000 and a sensitivity of 1.34 ns/με was obtained.

3.2 Curvature Sensing

The fibre-based CRD configuration presented in Figure 1 has also been used for the measurement of curvature (Silva *et al.*, 2015b). An OTDR is used to send impulses down into the fibre loop cavity (~800 m), inside of which a long period grating (LPG) is placed to act as sensing device. The LPG was written by UV in SMF28e with a period of 335 nm and a length of 25 mm. The LP07 resonance mode of the LPG is positioned at ~1566.2 nm with a full width half maximum (FWHM) of 33.7 nm. This resonance is situated in the long-wavelength side of the multimode laser spectrum which is centred at 1550 nm and has a 50 nm-bandwidth.

In this case, an added-signal was used for curvature sensing and it was obtained by the sum of several conventional CRD impulses. Figure 4 shows the CRD trace when the LPG was interrogated using (1) the CRD conventional signal processing and (2) when an added-signal was applied in the fibre loop.
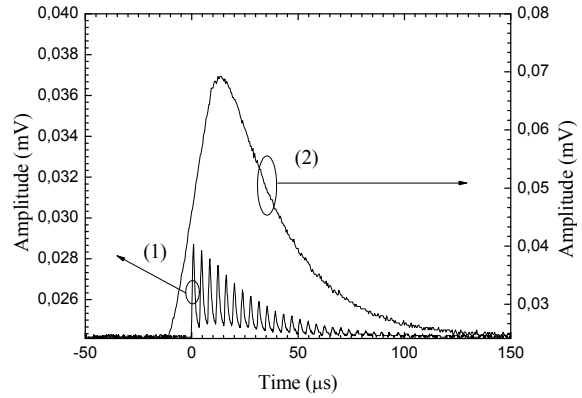

Figure 4: CRD trace for (1) conventional configuration and (2) added-signal obtained by the sum of several conventional CRD impulses.

In the first case (1), the OTDR sent impulses of 1 μs at 1550 nm down into the fibre cavity; the time of a single round trip was ca. 3.85 μs which is determined by the cavity length. An exponential fit was also performed and a ring-down time of 23.7 μs was attained, with an associated loop loss of 0.7 dB. In the second case (2), the OTDR sent impulses of 20 μs at 1550 nm in order to obtain the added-signal. After performing an exponential fit, a ring-down time of 43.3 μs was obtained. Such results show that the added-signal increases the optical power but increases as well the ring-down time due to the sum of the several loops that light travels inside the ring.

The behaviour of this structure as a curvature sensor was duly characterized. As expected, the amplitude of the added-signal decreases with decreasing curvature, as result of bending the LPG. The ring-down time as a function of curvature was also determined for both conventional CRD- and added-signals, as depicted in Figure 5.
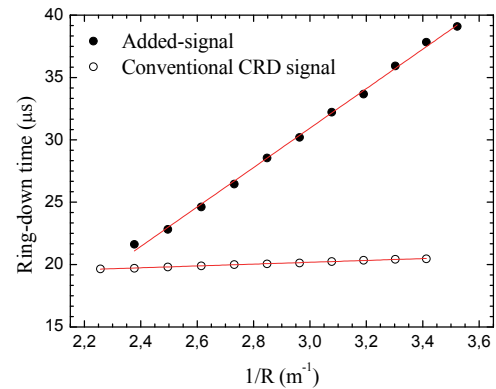

Figure 5: Ring-down time versus curvature applied to the LPG when interrogated by the conventional CRD signal processing and added-signal.

Results show that the sensitivities obtained for the added-signal and conventional CRD signal are 15.3 μs/m^{-1} and 0.74 μs/m^{-1}, respectively. The added-signal configuration presents a sensitivity 20-fold the one obtained for the conventional CRD signal processing.

3.3 Refractive Index Sensing

In a recent approach, a CRD system using a multimode interference (MMI) based fibre sensor was developed for refractive index (RI) sensing. Due to the high losses associated to the MMI-based sensing head, an erbium doped fibre amplifier (EDFA) was inserted in the fibre loop cavity for amplification of the output signal. The EDFA is composed by 2 m of an erbium-doped fibre (losses of 14 dB/m @ 980 nm) and in order to compensate the losses from the MMI-based sensing head, a current of 155.7 mA was applied to the fibre device.

The sensing head is based on multimode interference and relies on a singlemode – coreless-multimode – singlemode fibre configuration. The coreless-MMF is a pure silica fibre with 125 μm-diameter and 20 mm-length, which was spliced between two SMFs and interrogated in transmission.

The CRD trace obtained with the proposed configuration is shown in Figure 6. The time of a single round trip is ca. 7.8 μs and is strongly dependent on the pulse width, fibre length, fibre losses, MMI losses and others.
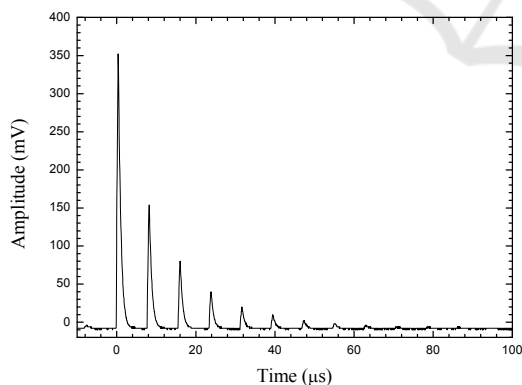

Figure 6: CRD trace for pulses sent by the modulated multimode laser source into the fiber loop with 500 ns width.

The sensing head was then submitted to RI changes of water caused by temperature variation. The MMI-based fibre sensor was placed under water and submitted to increasing temperature in the range 25–80°C. In this experiment, the OTDR sent impulses of 500 ns at the operation wavelength of 1550 nm, which in turn is located in the slope of the band-rejection filter centred at 1546 nm. Therefore, the wavelength variation caused by RI changes of the external medium will shift the band-rejection peaks, associated with an amplitude variation of the acquired signal. In this case, the temperature-induced RI variation of water causes the amplitude of the band-rejection peaks to change and consequently leading to measurable losses in the acquired CRD signal.

Figure 7 presents the ring-down time variation according to temperature-induced RI changes of water. Since the MMI-based fiber sensor is intrinsically sensitive to temperature but also to RI of the external medium, one had to remove the temperature component of the acquired output signal, in order to obtain the presented results.
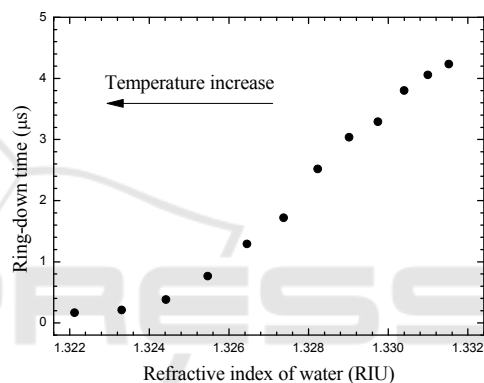

Figure 7. Ring-down time versus temperature-induced RI changes of water.

The behavior of the sensing head to temperature variation was studied. The MMI fiber sensor was placed in a furnace and submitted to increasing temperature and a negligible sensitivity of -1.6×10^{-9} μs/°C was attained. This allowed eliminating the temperature component from RI measurement of water and a linear sensitivity of 580 μs/RIU in the RI range of 1.324-1.331 was obtained.

4 CONCLUSIONS

This brief overview on fiber optic based CRD technique for sensing applications, undergone at INESC TEC, shows that one of the new lines of research is the use of existing equipment on the market for long range measurement. An example was recently demonstrated, namely, the use of the OTDR for the measurement of strain. Another line of investigation is signal processing that makes the

CRD a quick acquisition system and allows analysis in real time. The use of the add-signal as a new solution presents greater sensitivity when the sensor is subjected to curvature. Finally it was presented the use of the CRD for RI measurement. It is clearly that its application in the future will be in spectroscopy for medicine, biomedical and chemical areas of research.

ACKNOWLEDGEMENTS

REFERENCES

Berden, G., Peeters, R., Meijer, G., 2000. Int. Rev. Phys. Chem. 19, 565-607.

Herbelin, J. M., McKay, J. A., Kwok, M. A., Uenten, R. H., Urevig, D. S., Spencer, D. J., 1980. Applied Optics 19 (1), 144–147.

Anderson, D. Z., Frisch, J. C., Masser, C. S., 1984. Applied Optics 23 (8), 1238–1245.

Stewart, G., Atherton, K., Culshaw, B., 2004. Opt. Lett. 29 (5), 442-444.

Tarsa, W. P., Brzozowski, D. M., Rabinowitz, P., Lehmann, K. K., 2004. Opt. Lett. 29 (12), 1339-1341.

Ni, N., Chan, C. C., Dong, X. Y., Sun, J., Shum, P., 2007. Meas. Sci. Technol., Special Issue, 18, 3135-3138.

Silva, S., Passos, D. J., Marques, M. B., Frazão, O., 2015a. Microw. Opt. Technol. Lett. 57 (6), 1442-1444.

Wang, C., 2005. Opt. Eng. Lett. 44 (3), 030503.

Lerber, T., Sigrist, M. W., 2002. Appl. Opt. 41 (18), 3567-3575.

Silva, S., Biswas, P., Bandyopadhyay, S., Jorge, P. A., Marques, M. B., Frazão, O., 2015b. IEEE Photon. Technol. Lett. 27 (19), 2079-2082.

Wang, C., Scherrer, S. T., 2004a. Opt. Lett. 29 (4), 352-354.

Wang, C., Scherrer, S. T., 2004b. Appl Opt 43 (35), 6458-6464.

Qiu, H., Qiu, Y., Chen, Z., Fu, B., Chen, X., Li, G., 2007. Microw. Opt. Technol. Lett. 49 (7), 1698-1700.

Brown, R. S., Kozin, I., Tong, Z., Oleschuk, R. D., Loock, H.-P., 2002. J. Chem. Phys. 117, 10444-10447.

Tarsa, P. B., Wist, A. D., Rabinowitz, P., Lehmanna, K. K., 2004. Appl. Phys. Lett. 85 (19), 4523–4525.

Pu, S., Gu, X., 2009. Opt. Lett. 34 (12), 1774-1776.

Ni, N., Chan, C., Xia, L., Shum, P., 2008. IEEE Photon. Technol. Lett. 20 (16), 1351-1353.

Zhou, K. M., Webb, D., Farries, M., Hayes, N., Zhang, L., Bennion, I., 2009a. Opt. Lasers Eng. 47, 1023-1027.

Zhou, K. M., Webb, D. J., Mou, C. B., Farries, M., Hayes, N., Bennion, I., 2009b. IEEE Photonics Technol. Lett. 21 (22), 1653-1655.

Wang, C., Herath, C., 2010. Opt. Lett. 35 (10), 1629-1631.

Wong, W. C., Zhou, W., Chan, C. C., Dong, X., Leong, K. C., 2012. Sens. Actuat. B 161, 108-113.

Stewart, G., Atherton, K., Yu, H., Culshaw, B., 2001. Meas. Sci. Technol. 12, 843–849.

Vogler, D. E., Muller, M. G., Sigrist, M. W., 2003. Appl. Opt. 42 (27), 5413-5417.

Zhao, Y., Bai, L., Wang, Q., 2013. Opt. Communications 309, 328-332.

Shimizu, H., Noriyasu, H., 2014. Japanese J. Appl. Phys. 53, 116601.

Wang, C., 2009. Sensors 9 (10), 7595-7621.

Ye, F., Qi, B., Qian, L., 2011. Optics letters 36 (11), 2080-2082.

Hiraoka, T., Ohta, T., Ito, M., Nishizawa, N., Hori, M., 2013. Japanese J. Appl. Physics 52 (4R), 040201.

Passos, D. J., Silva, S. O., Fernandes, J. R. A., Marques, M. B., Frazão, O., 2014. Photonic Sensors 4 (4) 295-299.

Silva, S., Marques, M. B., Frazão, O., 2016. Microw. Opt. Technol. Lett. 58 (11), 2711-2713.